Worldwide Effectiveness of Various Non-Pharmaceutical Intervention Control Strategies on the Global COVID-19 Pandemic: A Linearised Control Model

Joshua Choma[1], Fabio Correa, PhD[5], Salah-Eddine Dahbi, PhD[1], Barry Dwolatzky, PhD[4], Leslie Dwolatzky[3], Kentaro Hayasi[3], Benjamin Lieberman[1], Caroline Maslo, MD, PhD[6], Bruce Mellado, PhD[1,2], Kgomotso Monnakgotla[1], Jacques Naudé[7], Xifeng Ruan, PhD[1], Finn Stevenson[1]

Abstract

Background COVID-19 is a virus which has lead to a global pandemic. Worldwide, more than 100 countries have imposed severe restrictions regarding freedom of movement amongst their citizens in a bid to slow the spread of the virus. These restrictions, which are part of a set of non-pharmaceutical interventions, have recently been classified by the Oxford COVID-19 Government Response Tracker (OxCGRT) team and a nominal index measure has been defined for use by the wider international community. We address the use of this index measure to establish the degree and characteristics of control of the transmission rate of the virus within a representative sample of countries in the World and states in the United States of America.
Methods Country specific, Susceptible-Infected-Recovered-Deaths (SIRD)

[1]School of Physics and Institute for Collider Particle Physics, University of the Witwatersrand, Johannesburg, Wits 2050, South Africa
[2]iThemba LABS, National Research Foundation, P.O. Box 722, Somerset West 7129, South Africa
[3]School of Computer Science and Applied Mathematics, University of the Witwatersrand, Johannesburg, Wits 2050, South Africa
[4]Joburg Centre for Software Engineering, University of the Witwatersrand, Johannesburg, Wits 2050, South Africa
[5]Department of Statistics, Rhodes University, Grahamstown 6139, South Africa
[6]Department of Quality Leadership, Netcare Hospitals, Johannesburg, South Africa
[7]working in association with Biomedical Engineering Research Group, School of Electrical and Information Engineering, University of the Witwatersrand, Johannesburg, South Africa

models with latent dynamics were constructed using publicly available data for 23 countries and 25 states of the United States of America. Each of the models were linearised and classical frequentist error propagation was applied to them individually. The time varying, observable model parameters were extracted for each day that data was made available. The OxCGRT stringency index, p, was used to regress against these model parameters. The regression of the transmission rate as a function of p in each locale was through a linear parameter α_s. In addition, macroscopic indices from the World Bank were used to explore inter-country variation in the measured parameters.

Results The world average was $\alpha_s = 0.01$ (95% CI 0.0102 - 0.0112) with an ensemble standard deviation of 0.0017 (95% C.I. 0.0014 - 0.0021), strongly indicating a universal behavior. While lockdown measures have been successful in curbing the spread, our study indicates that removing them too swiftly will result in the resurgence of the spread within one to two months. Reducing the stringency index by 10 will delay reaching the apex by about 6 months, where reducing it by 20 will delay by only four months. During the post-lockdown period it is essential to increase α_s. For the system to remain sub-critical, the rate with which α_s increases should outpace that of the decrease of the stringency index. The spread of the virus is found to be insensitive to the Gini index and other socio-economic indexes. The typical adjustment time to see the effects of control, b_r^{-1} varied between 1.49 days for Peru and 38.09 days for Sweden. In the United States, the typical adjustment time to see the effects of control, b_r^{-1} varied between 1.41 days for Colorado to 15.91 days for Ohio.

Interpretation Given the measured characterisations of each locale, the effects of any change in non-pharmaceutical intervention may be anticipated and predictions can be made regarding the possible case load which is specific to that environment. This is accomplished by specifying an acceptable level of transmission, β_f, given the prevailing economic and social constraints which uniquely determines an overall stringency of intervention level p. As a policy maker, there are possible intervention combinations to choose from and a combination must be selected that achieves p or greater.

Keywords: COVID-19, Model, Control

---

1. Introduction

A novel corona virus, named COVID-19, was detected in the Hubei province of China in late December 2019 and rapidly spread resulting in a confirmed global pandemic by 11 March 2020[1]. As at 26 April 2020, the total number of infections has exceeded 3.1 million confirmed cases with more than 210 thousand deaths worldwide attributable to the effects of the virus[2]. A large, worldwide modeling effort is currently underway to improve health policy decision making with regards to the COVID-19 pandemic[3–7]. Many research groups and national response teams have looked into country specific intervention strategies[4,6–10].

The insight our research offers is a worldwide survey of the dynamics and characteristics various countries possess with regards to the control of the pandemic, through non-pharmaceutical interventions (NPI)s. We have used sufficient statistics and a mechanistic model with latent dynamics and error propagation to classify the dynamic behaviour of each country for which data is available. This means that characteristic variations between (and within) countries are comparable for the first time. The purpose is to allow policy makers to gradually control their local epidemic within their contextual situation without having to rely on the parameters derived from other country-specific intervention studies.

2. Method

For a fair comparison of the effect of interventions, carefully curated, comprehensive and frequently updated data is a requirement. Data was, therefore, sourced from the John's Hopkins COVID-19 data repository because it fulfilled both the due diligence and frequency of updating needed for this research[11].

Using this existing data up to and including 26 April 2020, multiple SIRD with latent dynamics and error propagation models were employed to capture the salient features of the present pandemic within each country for which reliable information was available. The chosen modeling method is far simpler than some of the most comprehensive models employed during this pandemic[7,8]. Its simplicity is its strength and the model is 'mind-sized'; it has a number of sufficient statistics which entirely capture the models behaviour and allow for measurement of the efficacy of control measures on the key variables of interest for policy makers and public health authorities.

Moreover, these parameters may be compared between and within countries. Individual based models cannot do this at a global scale without being properly calibrated and sufficient statistics being defined.

An initial cohort of 23 countries and 25 states within the United States of America were chosen to be as representative and diverse as possible. These countries and states have implemented a wide variety of non-pharmaceutical intervention strategies. Both timing and level of interventions were fairly represented in this cohort.

Levels of control were measured by the Oxford COVID-19 Government Response Tracker (OxCGRT) stringency index[12]. This index, denoted p in our work, takes values from 0 to 100 and is indicative of the severity and number of discrete measures that have been taken to try to curb the spread of COVID-19. It is sensitive enough to differentiate between situations where an intervention measure is suggested by government but not enforced[12].

At the time of writing; America did not have a stringency index published. A best fit, using the methodology in Hale et al. [12] and publicly available coarse grained intervention information, was employed to align the results. This is described fully in Appendix A.

Daily parameter estimates of the models were extracted from the data using a least-squares framework and candidate kernel functions were regressed on the daily parameter estimates. These kernel functions represent the time domain response of a model parameter to a given level of control and are based on dynamic hypotheses regarding the time evolution of the parameters in response to the NPI changes which are measured with the OxCGRT stringency index.

Given the large scale, the dynamic hypotheses were generated by the recognition that additive effects of random variables contribute to the time domain behaviour of the effects of intervention; this is the reason for the prominence of the exponential approach a hypothesised steady state (for constant NPI level)[13].

This sort of exponential behaviour will cease to be representative if there is a systematic breakdown in roll-out of the interventions; i.e. there exist delays which should be modeled with random variables that have poorly defined variance (so called 'fat tails')[14]. If such a systematic breakdown in roll-out were to happen, our proposed control model would cease to be valid.

2.1. Model

The characteristics of the present pandemic are atypical, a key fact that is difficult to capture directly with the classic deterministic differential equations of epidemiology is that infected individuals may be asymptomatic and infectious[15].

An SIRD (with latent dynamics) is one of the simplest models which captures the essential features of the present COVID-19 outbreak and allows for clear interpretation with regards to control and decision making. This model is depicted in Figure 1 and has several key parameters which summarise the evolution of the disease, in sympathy with situations which admit the existence of sufficient statistics which completely characterise the behaviour of a random variable[13].

The latent dynamics are essential to capture the following clinical properties of COVID-19:

1. Asymptomatic cases are infectious[16,17].
2. It is possible for deaths to be overstated since positive tests are not a requirement in some locales for establishing the basic underlying cause of death in this pandemic; reasonable clinical judgement is[18]. In addition, overstatements in clinical cases may be due to the highly infectious nature of the virus; patients with severe co-morbidites may not necessarily die with the virus as the basic underlying cause even though it is likely to be present in the patient if they are admitted to a facility with many active COVID-19 cases.
3. There are early reports that the latent prevalence (using a seroprevalence study) may be as high as 14% of one of the most densely populated cities in the World[19].
4. There have been serious calls for protection of front-line health care workers as a result of early experiences with the epidemic[20,21]. The nosocomial infections within hospital care providers as a group may be non-negligible, though for the large scale model we are considering, this group has not been partitioned separately.

The observable (directly measurable) dynamics capture the standard features of susceptible portions of the population becoming infected and then either recovering with perpetual immunity or dying.

There is evidence that relapse is possible, where recovered patients would become susceptible again[22]. This model variation has not been explicitly

considered because do not know the significance of this yet; it is possible that these are people who were not fully cured[22], they may have been reinfected with a different strain[17], the reverse transcription polymerase chain reaction (RT-PCR) test can give a positive result due to extracellular RNA, shedding of non-viable virions etc.

Of note is that the implicit assumption with this approach is that there is a single viral strain which is being modelled. If there are multiple strains, each of which is observable and differentiable through specialised testing then refinements on the labelling and parameters are possible.

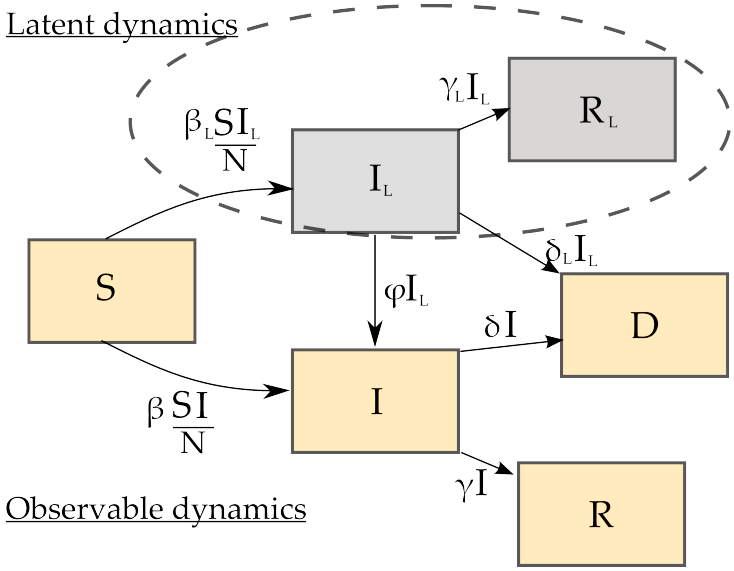

Figure 1: SIRD model with Unobserved Latent Dynamics.

2.2. Observable Dynamics

Under the stated clinical conditions which limit nosocomial infections through effective monitoring and personal protective equipment use; the transmissions between known infected patients and susceptible individuals (in the broadest sense possible) should be rare. The typical disease progression time frame[15,23] implies that latent infections leading to deaths should be rare, it is presumed that patients with severe symptoms are brought in for treatment. Under these conditions the latent dynamics in the model simplify

with $\delta_L \approx 0$ and $\beta \approx 0$ and this mode simplification is used throughout. What is observed then, in terms of increase in measured infections I, is achieved strictly through ϕI_L. These are the detected infections and dependent on the detection rate, ϕ, and test efficiency. The modeling assumption of effective known positive patient quarantining means that new infections must be latent, initially. Said another way, susceptible patients, S, are infected through interaction with latent infected individuals, I_L and these new latent infections are detected, I in a way which is dependent on the daily observed infection rate ϕ.

2.3. Daily observed infection rate, ϕ

The daily observed infection rate is related to the efficiency of the testing procedure, the number of tests which are conducted, the fraction of those carrying the virus who present with symptoms (in order for them to be considered for testing) and a few other factors besides.

The units of ϕ are *observed infections per latent infection per day.*

An important component for estimating ϕ is the number of positive individuals who do not know their status and are asymptomatic. Random testing has proven useful in this regard in Iceland[17] and New York[19]. Exhaustive testing was possible in the small populations in the municipality of Vo, Italy and on the Diamond Princess cruise ship with each study including more than 3,000 individuals.

Reliable estimates of asymptomatic cases due to either extensive randomised testing or exhaustive testing in closed populations are presented in Table 1. Unfortunately, the number of asymptomatic cases are approximately 50% of all positive COVID-19 patients. The fraction of asymptomatic cases in enclosed populations, the number of patients with antibodies present (due to randomised population seroprevalence studies) and patients with symptoms who are subclinical and do not warrant admission and formal testing will also all influence the rate measured by ϕ.

2.4. Kernel functions

The roll-out of any country-wide control measure is subject to random variations in timing and levels of civil compliance dependent on the execution plan and the populace's disposition. To capture these stylised facts, there is a typical adjustment time associated with a country-wide lock-down which is unique to that country.

Study	Asympt. positive tests
Diamond Princess[15][n=4,062]	55% (95% CI 52%-59%)
Vo Italy[24][n=3,300]	50% - 75%
Japanese nationals evacuated[25] [n=565]	31% (95% CI: 7.7% - 54%)
Nursing home, Washington[26] [n=23]	43% (95% CI 26% - 63%)
Iceland (Open Invite)[17] [n=10,797]	41% (95% CI 32% - 52%)
Iceland (Random)[17] [n=2,283]	54% (95% CI 30% - 77%)
Northern Italy blood donors[27] [n=60]	66% (95% CI 54% - 77%)

Table 1: Results from various studies regarding the number of asymptomatic cases amongst those testing positive for COVID-19.

This was modeled with the kernel function, conditioned on the control measure p:

$$\beta_p(t) = \left(1 + b_0 e^{-b_r \Delta t}\right) \beta_f(p), \tag{1}$$

where $\beta_f(p)$ is the asymptotic value of the observed daily transmission rate, b_r is the typical adjustment rate and b_0 is used to model the initial transmission rate before the control p is applied. A characteristic plot is depicted in Figure 2.

As a starting point, it is hypothesised that the typical adjustment rate b_r is characteristic of a nation and that $\beta_f(p)$ is dependent on the stringency of control p through:

$$\beta_f(p) = \beta_0(1 - \alpha_s p), \tag{2}$$

where α_s is the effect of stringency on transmission rate.

The kernel function for $\gamma(t)$ is:

$$\gamma_p(t) = \gamma_0, \tag{3}$$

regardless of control. The clinical and physical justification for this model is that the inherent properties of the recovery process do not change with non-pharmaceutical control, assuming the hospital system has not been overwhelmed yet.

The kernel function for $\delta(t)$ is:

$$\delta_p(t) = d_0 t^{d_1} e^{-d_r \Delta t}, \tag{4}$$

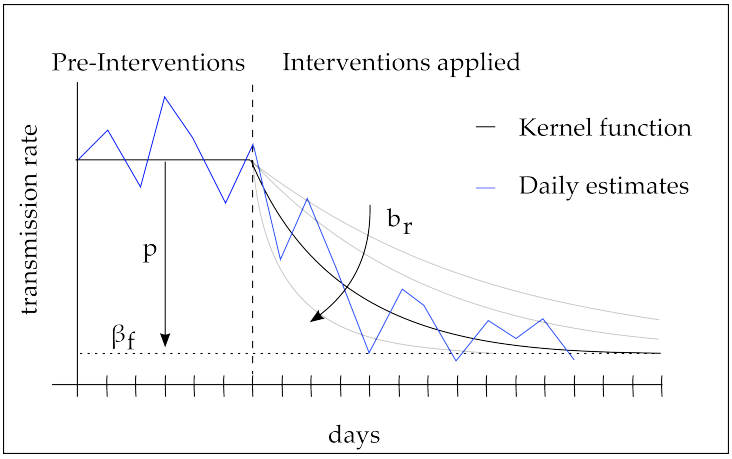

Figure 2: The transmission rate kernel function depicting the typical adjustment rate, b_r and final transmission rate β_f. The control index p affects the total reduction in transmission.

which is the result that would be theoretically expected from a cascade of first order processes[28]. The temporary increase in this parameter is due to the reduced number of severe infections which will artificially raise it since $\delta \propto I^{-1}$, see (B.7). This function captures the transients inherent in the daily death count as a result of intervention only. The steady state value which is asymptotically approached as the epidemic reaches steady state.

2.5. Control

The capacity of countries to properly address the risk that COVID-19 poses is varied; with less than half being fully positioned to prevent, detect, and respond appropriately[29]. The World Health Organisation identifies as a key strategic objective within the current global pandemic, the need to reduce human-to-human transmission of the virus[2]. Further, the WHO recommends combinations of public health measures which would jointly work to achieve this such as rapid identification of infections, contact tracing, infection prevention and control at healthcare facilities, additional health measures for traveling to name a few[2].

A feasibility study of contact tracking and tracing in the UK was established using the known basic reproductive number, various initial conditions and various successful traces[6]. The results were that a prolific disease with a high R_0 required a large percent of traces to be found[6].

Of note is that the basic reproductive number depends on the conditions under which it is measured; it has been proven that various interventions bring down the basic reproductive number and these would make the feasibility of tracking and tracing more attractive. In addition, tracking and tracing is known to reduce the basic reproductive number further (see Singapore and Taiwan).

These results are well known in non-linear feedback system theory; interventions taken all contribute to make the control of the disease easier since they change the system parameters[30]. In a very real sense, COVID-19 under intervention is not the same (from a systems perspective) as COVID-19 without intervention; they each have their own dynamics and this makes control of one fundamentally easier than the other.

In terms of the proposed latent dynamics model, the effect of various control policies are depicted in Figure 3. This Figure clearly demonstrates the value of the proposed methodology; one may holistically view the epidemic and various policy actions in a single framework and be able to anticipate the consequences.

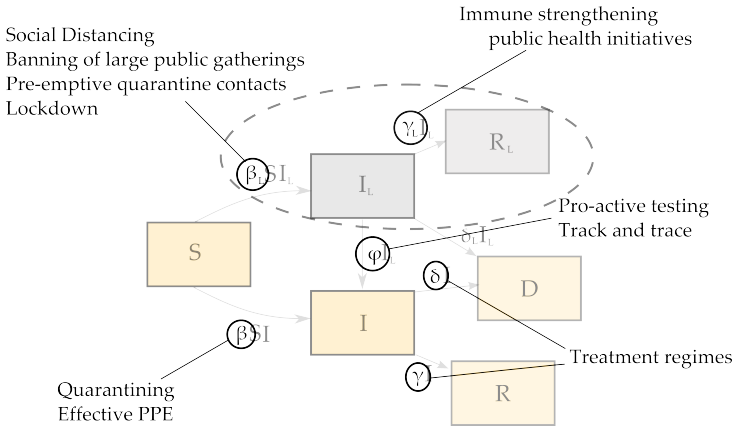

Figure 3: The Effects of Various Interventions on the Model

2.6. NPIs and the OxCGRT Stringency Index

The OxCGRT has developed a valuable database for comparing countries response strategies.[31] The database contains the following levels of control (coded using ordinal numbers) and timing for 139 countries:

1. S1 - School closure
2. S2 - Workplace closure
3. S3 - Cancel public events
4. S4 - Close public transport
5. S5 - Public information campaign
6. S6 - Domestic travel bans
7. S7 - International travel bans

Also included in this data set is a Stringency Index, p in our notation, which provides a single number that captures the overall level of intervention implied by combinations of the ordinal numbers S1-S7. The Oxford stringency index is calculated using a weighted average of the above seven non-pharmaceutical interventions[32].

These interventions were rolled-out at different times for different levels depending on the number of days since the first reported case.

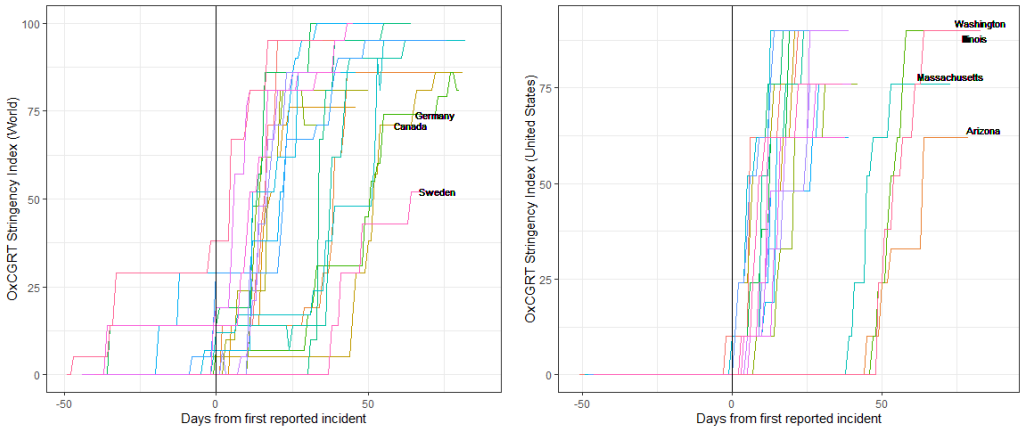

Figure 4: Timing and Severity of NPIs in the set of representative countries and US

Recovery rate

The kernel in (3) is effectively stating that the daily recovery rate is constant, in the absence of improved clinical treatment regimes or viral physiology (the virus has not sufficiently mutated so that its resolution time has been substantially altered within the population under consideration). Since the control measures considered, p are all non-pharmaceutical, the recovery rate

dynamics are dictated by $\gamma(t) = \gamma_0 = const.$, whatever the value of p. This is true provided that the health care system has not been overwhelmed; which is the purpose of the control system.
In the absence of data on the population dynamics during withdrawal of some NPI's, our model is conservative and uses the same typical adjustment rate for the withdrawal of NPI's as for the addition of NPIs.

3. Results

The research output, using the foregoing methodology are shown in Table 2 for various countries and in Table 3 for various States of the US. Results are expressed in terms of γ_0, d_0, β_0, b_r^{-1}, p_{max} and α_s in Table 2. Table 3 does not display γ_0, as the data for the number of recoveries has not been reported since late March.

The first salient feature of Tables 2 and 3 is that the evolution of the pandemic in different countries share strong similarities. Some variations are observed in the parameters γ_0, d_0, β_0, where b_r^{-1} is subjected to features of the data most likely to specifics in the reporting.

The most important result from Tables 2 and 3 revolves around the observation that the bulk of countries and US States display values of $\alpha_s \approx 0.01$. It is remarkable that this occurs whilst other parameters are measured to have a great variety, especially β_0. This striking result also speaks to the universal character of the stringency index used here to quantify NPIs. This observation will be reinforced by results reported in Section 4.3, where the rate of spread does not seem to depend on socio-economic factors but rather on the fraction of the population in large cities.

The results of α_s display some deviations from the average value, especially in some States of the US. Section 4.4 will touch upon an analysis of these outliers and how these appear to be related to population sparsity.

4. Discussion

4.1. Predictive capabilities of the model

The primary intent of this paper is to provide a framework with which to issue country-specific predictions for the temporal evolution of the spread and other outcomes in the post-lockdown period (for a variety of control policies). A few weeks of containment measures have yielded valuable data across the World to understand the observable dynamics, where the latent

Country	γ_0	d_0	β_0	b_r^{-1} [days]	p_{max}	α_s
Austria	0.045	0.00342	0.26	7.15	95	0.010
Belgium	0.019	0.00070	0.24	19.12	86	0.012
Brazil	0.034	0.01670	0.39	2.97	76	0.009
Canada	0.026	0.00333	0.31	13.53	86	0.010
Chile	0.036	0.00150	0.30	5.74	81	0.009
Ecuador	0.006	0.00004	0.42	2.89	100	0.009
Egypt	0.027	0.00058	0.15	9.18	100	0.005
France	0.019	0.00012	0.33	0.07	95	0.011
Germany	0.042	0.00258	0.28	10.50	86	0.011
Ireland	0.015	0.00372	0.34	23.46	86	0.012
Israel	0.018	0.00003	0.27	8.89	100	0.009
Italy	0.020	0.00107	0.24	10.26	95	0.010
Morocco	0.011	0.0021	0.25	16.58	86	0.010
Netherlands	0.001	0.00050	0.22	16.21	86	0.012
Peru	0.051	0.00163	0.33	1.49	86	0.007
Portugal	0.002	0.00045	0.31	8.28	100	0.009
South Africa	0.018	0.00050	0.28	2.19	100	0.008
South Korea	0.032	0.00031	0.07	16.24	81	0.012
Spain	0.037	0.00006	0.34	11.96	95	0.010
Sweden	0.003	0.00002	0.12	38.09	52	0.019
Switzerland	0.036	0.00045	0.46	8.12	81	0.012
Turkey	0.012	0.00047	0.64	14.41	95	0.011
UK	0.001	0.00027	0.23	14.37	71	0.013

Table 2: Results for various representative countries around the World. Results are given in terms of γ_0, d_0, β_0, b_r^{-1}, p_{max} and α_s (see text). Parameters have been obtained with data up until April 26 2020.

dynamics are significantly less understood. The framework proposed here allows for the modeller to factorise latent and observable dynamics, with the intent to address the evolution of the latter without major hindrance from limited knowledge of the former. In this setup the temporal evolution of observable dynamics are weakly coupled to that that of the latent dynamics through the term ϕI_L (see Figure 1). In practice, the presence of this term implies that the total population of observed infections will be bound by the parameter ϕ, which can be viewed as the fraction of true infections that

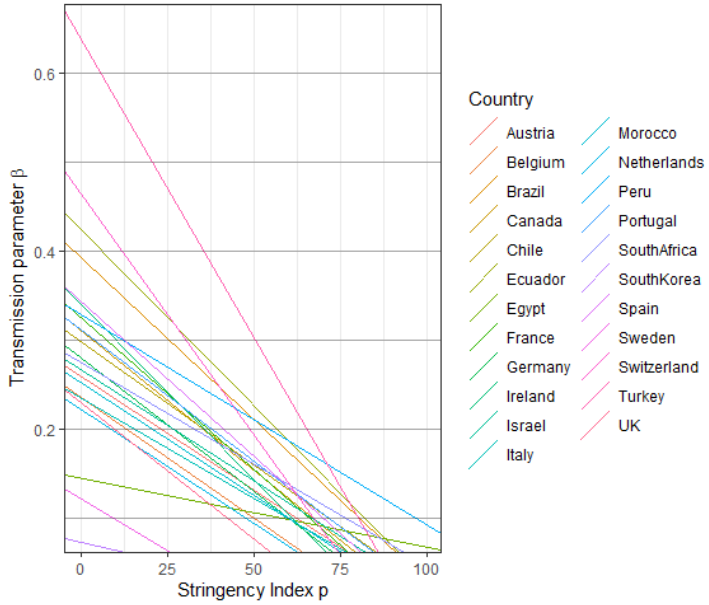

Figure 5: Implications of the model on observed transmission rate and stringency index for representative countries.

become symptomatic enough to warrant testing and, therefore, become classified as an observed infection upon a positive result. Provided that $\gamma \leq \gamma_L$ the maximum number of observed infections will be limited to ϕN.

The temporal evolution will depend on the initial parameters relevant to the spread and the parameters that are chosen to depend on time. For illustration purposes, we chose to freeze d to the last values measured, or d_0, as reported in Tables 2 and 3.

From Eqs. 1 and 2 one gets for the post-lockdown period:

$$\beta(t,p) = \beta_f - (1 + e^{-b_r t})\beta_0 \alpha_s \Delta p, \tag{5}$$

where $t = 0$ corresponds to the end of the lockdown period and the enacting of new interventions, such that $p < p_{max}$. The implementation of new less restrictive measures will yield $\Delta p = p - p_{max} < 0$, where $\beta(t,p) > \beta_f$. It is reasonable to infer that the typical adjustment time leading to the asymptotic value of β_f may also apply here.

For illustration purposes, we choose the configuration of parameters obtained with Italian data, where $\phi = 0.1$ is used (see Section 2.2. The scenario

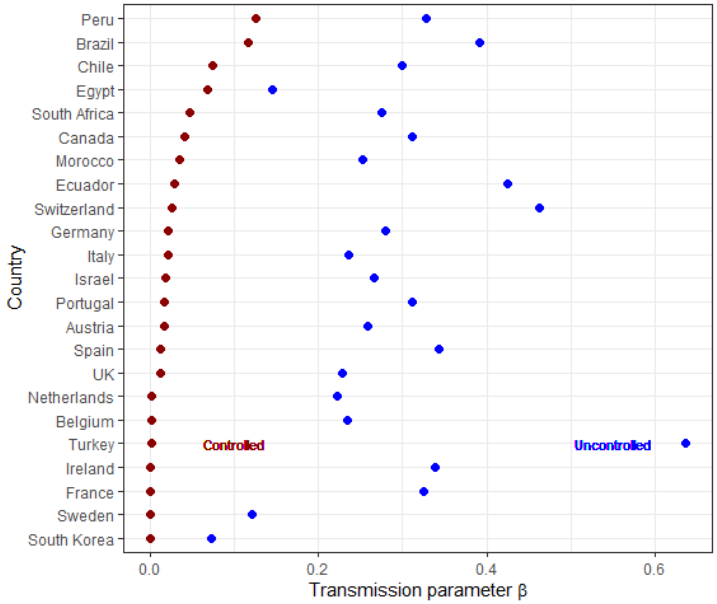

Figure 6: Effect of NPIs on the transmission rate parameter in the set of representative countries (ordered by β_f)

considered here assumes that variations of the index occur after the last available data with $\Delta p = -10, -30$. Figure 9 the time dependence of the number of symptomatic population, the active cases and the cumulative number of cases and fatalities. One can appreciate that going from $\Delta p = -10$ to $\Delta p = -30$ has serious consequences in terms of the time it takes to achieve the peak in active case as well as the amplitude of the peak. This is further illustrated in Figure 10, where the number of active cases and daily fatalities are shown as a function of time for different Δp ranging from -10 to -50. One can appreciate the swift change in the in the dynamics when going form $\Delta p = -10$ to $\Delta p = -20$, where the time required for the peak to occur would go from over six months to about four and where the amplitude of the peak would increase by a factor of two.

Two main sources of uncertainty are considered here. The leading source stems from the variation of the parameter α_s. The statistical error of α_s are of order of few % depending on the country. Here a more conservative approach is adopted. The country-to-country variation, which is of order of 10%, as discussed in Section 4.5, is considered to be a more realistic estimate of the potential deviation from the linear behavior assumed in Eq. (2). A

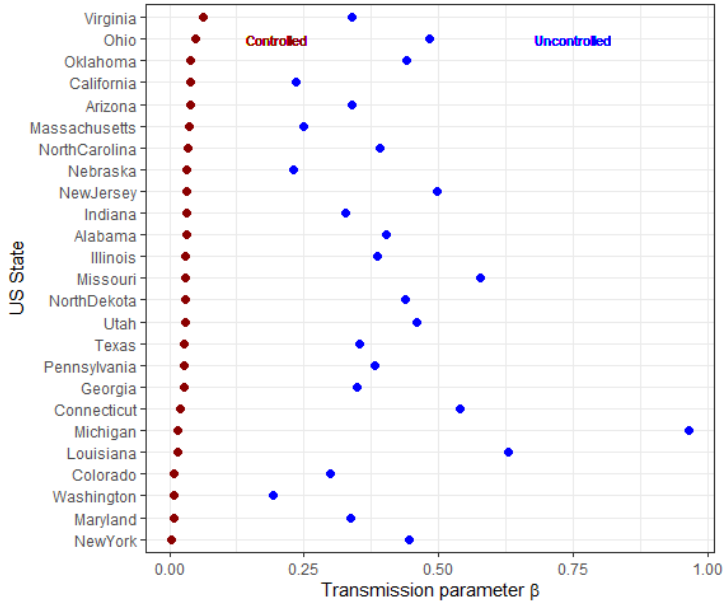

Figure 7: Effect of NPIs on the transmission rate parameter in the US (ordered by β_f)

sub-leading source of uncertainty is related to the uncertainty in the determination of γ_0, the daily recovery rate. This second source is much smaller in the Italian case compared to that assumed for α_s. Graphs in Figure 9 display the bands that incorporate the uncertainties described here.

Results shown in Figures 9 and 10 speak to the importance of a phased approach during the post-lockdown period. Swiftly releasing containment measures would lead to the resurgence of very large peaks of symptomatic infections within a month or two, leading to even worse outcomes compared to those observed so far.

4.2. Inequality for Sub-critical Behavior of the System

It will be argued that one of strategies for the post-lockdown period is to increase α_s as p decreases in order to sustain quasi-linear behavior in the time evolution of the number of active cases, as seen in Figures 9 and 10 for $\Delta p = -10$. In practice, all relevant parameters that enter the temporal evolution described above need to be tuned such that the expected peak of the number of cases and ICU usage falls below the thresholds characteristic to each country. One can denote a vector of critical parameters for which a

Country	d_0	β_0	b_r^{-1} [days]	p_{max}	α_s
Alabama	0.00074	0.40	9.01	90	0.011
Arizona	0.00009	0.34	5.88	62	0.014
California	0.00093	0.23	10.56	90	0.010
Colorado	0.00011	0.30	1.41	90	0.011
Connecticut	0.00057	0.54	12.19	76	0.013
Georgia	0.00015	0.35	15.53	76	0.013
Illinois	0.00036	0.39	9.20	90	0.010
Indiana	0.00127	0.33	5.99	90	0.010
Louisiana	0.00044	0.63	5.59	90	0.011
Maryland	0.00282	0.34	10.66	90	0.010
Massachusetts	0.00251	0.25	8.98	76	0.011
Michigan	0.00102	0.97	8.11	90	0.011
Missouri	0.00003	0.58	3.45	76	0.012
Nebraska	0.00079	0.23	3.12	62	0.013
New Jersey	0.00002	0.50	8.20	90	0.011
New York	0.00006	0.45	10.71	90	0.011
North Carolina	0.00131	0.39	9.49	90	0.010
North Dakota	0.00022	0.44	10.04	48	0.018
Ohio	0.00066	0.48	15.91	90	0.011
Oklahoma	0.00025	0.44	4.75	76	0.012
Pennsylvania	0.00005	0.38	6.81	90	0.010
Texas	0.00009	0.35	8.17	76	0.012
Utah	0.00049	0.46	4.86	62	0.015
Virginia	0.00135	0.34	5.38	76	0.011
Washington	0.00035	0.19	5.50	90	0.010

Table 3: Same as Table 2 for various States of the United States.

country's healthcare system is not overwhelmed:

$$\vec{v}_c(t) = (\gamma_c, d_c, \beta_c, \alpha_s^c). \tag{6}$$

One can assume that γ_c and d_c display a weak time dependence in that they primarily depend on medical advances, rather than on policy interventions. In this setup the condition for the system to remain sub-critical can

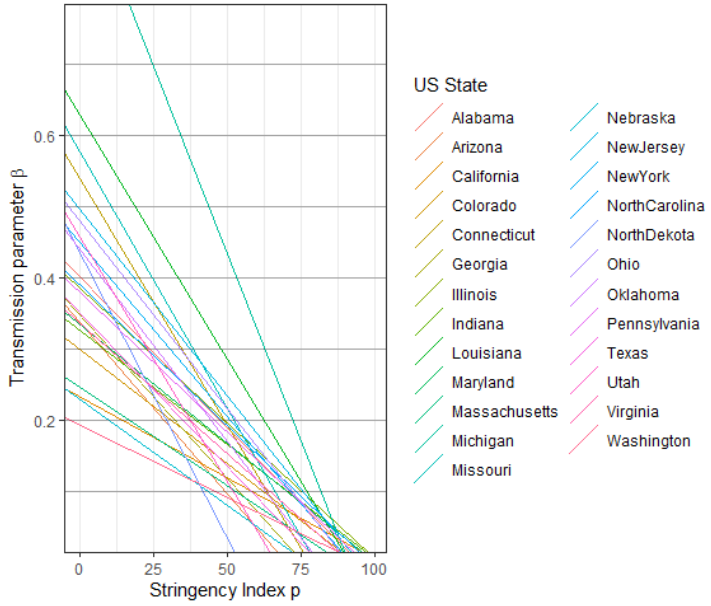

Figure 8: Implications of the model on observed transmission rate and stringency index for selected states in the US.

be expressed as follows:

$$\left.\frac{\partial \alpha_s}{\partial t}\right|_c \geq -\left.\frac{\partial p}{\partial t}\right|_c, \tag{7}$$

where the temporal partial derivatives are evaluated at the point of criticality defined by $\vec{v}_c(t)$. The inequality 7, while seemingly straightforward from the mathematical standpoint, it has serious consequences for policy makers. While lockdown measures have been successful in bringing the reproductive factor down to one and below, it is evident that these are having devastating effects on the economic landscape. In African countries, lockdown measures necessary to control the epidemic are leading to widespread malnutrition in vast sections of the population. On the other hand, the illustrative example shown in Section 4.1, indicates that for fixed α_s, reducing p significantly would lead to the advent of an epidemic of unprecedented proportions. Under these conditions, the inequality 7 speaks to the need to ensure that the rate with which α_s grows should outpace that of easing non-pharmaceutical interventions. Governments, policy makers and society as a whole need to embark in a titanic effort to increase α_s by all means. Strict adherence to social distancing and other advisories is paramount for this endeavor to suc-

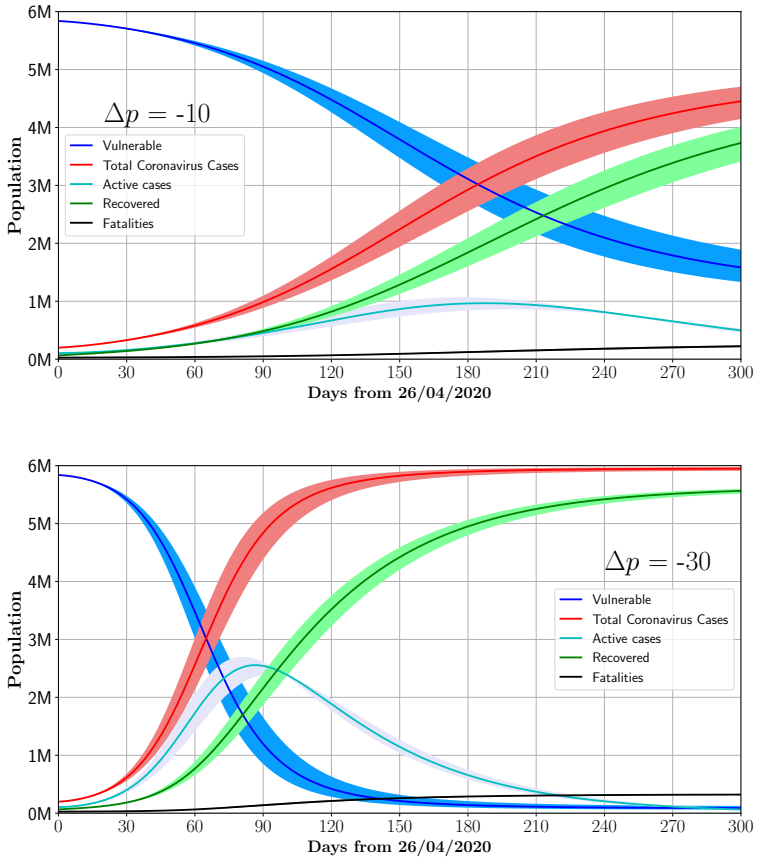

Figure 9: Post-lockdown scenarios for Italy for $p = 85$ (upper plot), $p = 65$ (lower plot). Results are given using $\phi = 0.1$ of the susceptible population population, or vulnerable population, active cases and the cumulative distribution of total cases and fatalities. The bands correspond to the uncertainties in the model (see text).

ceed. Careful monitoring will also pivotal as ever during the post-lockdown phase. Particular attention needs to be given to the temporal evolution of α_s.

4.3. Correlation with Macroscopic Indexes

The phases of the spread and its parameters bear strong similarities in a wide range of countries considered here. However, non-trivial differences in terms of parameters can be observed when scrutinising country by country variations. It is relevant to correlate variances with respect to macroscopic

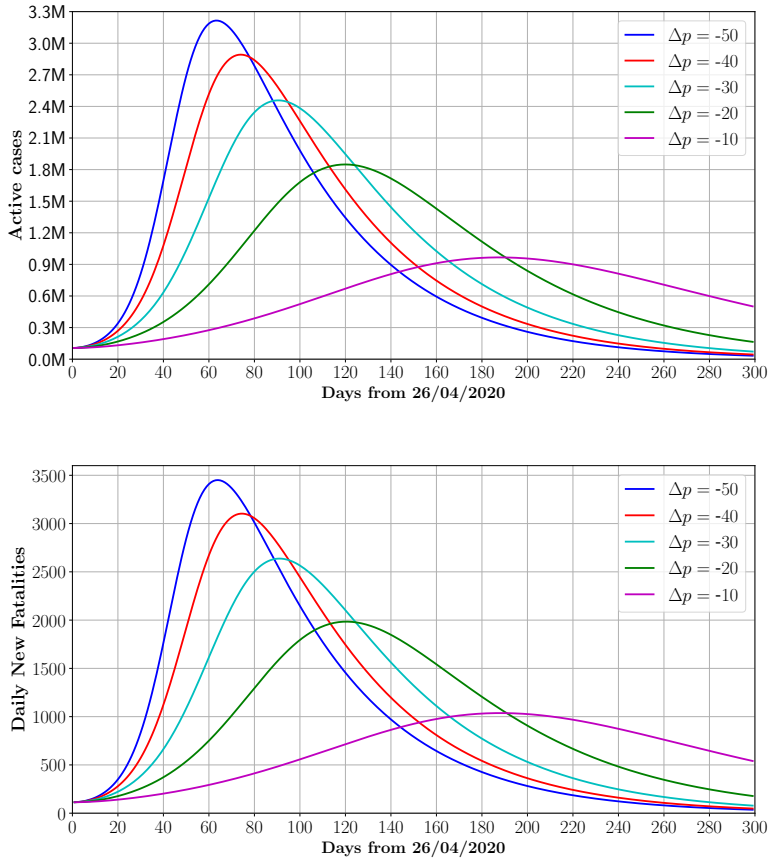

Figure 10: Number of active cases and new fatalities as a function for time for Italy by assuming different values of Δp ranging from -10 to -50. Results are computed with $\phi = 0.1$.

indexes. For this purpose the number positive cases is analysed as a function of time using the parametric expression:

$$I(t) = \frac{I_{tot}}{1 + e^{-\xi_I (t-C)}}, \tag{8}$$

where I_{tot} denotes the total expected number of positive cases for $t \to \infty$, ξ_I is the slope of the exponential growth that characterises the first phase of the spread, and C can be interpreted as a measure of the time needed to deviate from the initial exponential growth leading to containment. Time is expressed in number of days. A total number of 67 countries are selected,

where containment measures have proven effective in curbing the spread. These include countries in all continents and with a wide span in terms of socio-economic development, inequality and population density.

Macroscopic indicators are organised according to relevant themes: socio-economic vulnerabilities, demographics, social expenditures and aggregate economic indicators. A total of 34 indicators from the World Bank data base are selected and are correlated with the parameter ξ_I from each country.

The Gini index quantifies the extent to which the distribution of income among individuals or households deviates from perfect equality. The selected sample of countries displays a minimum and a maximum Gini index of 24 and 50, respectively. It is found that the parameter ξ_I is almost insensitive to the Gini index. This is illustrated in Figure 11 where the red line correspond to a first order polynomial that is consistent with zero slope. In order to exclude statistical fluctuations in the sample a similar study is performed using the percentage share of income held by the lowest 10% and 20% of the income bracket. No significant correlation is found for either of the indexes. This indicates that social inequality is not strongly correlated with the rate of spread of the virus.

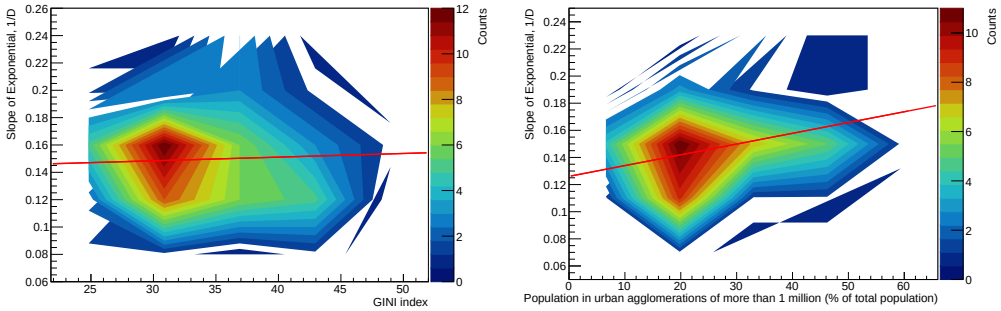

Figure 11: Correlation of ξ_I (see text) with the Gini index (left) and the population in urban agglomerations of more than one million to the country's population living in metropolitan areas (right). The red lines correspond to first order polynomials that illustrate the degree of correlation.

This observation is further strengthened by evaluating the correlation with the proportion of the urban population living in slum households. According to the World Bank, a slum household is defined as a group of individuals living under the same roof lacking one or more of the following conditions: access to improved water, access to improved sanitation, suffi-

cient living area, and durability of housing. Out of the 67 countries under scrutiny, 18 report a significant fraction of urban population living in slums. In this sample of countries the fraction ranges from 8% to 53%. No significant correlation is found between this index and ξ_I. In addition, the average value of ξ_I for these 18 countries is compatible with that of the rest of the ensemble studied.

As per the physical picture underlying the model used to describe the spread, it is expected that population density should play a significant role. No significant correlation is found with the average population density. This can be explained by the fact that the average population density is not necessarily a good metric for population density in urban areas, where the spread is most likely to occur. It should be noted that the correlation with the fraction of the population in urban areas is not statistically significant. In order to scrutinise the relevance of localised population density, the index made of the population in urban agglomerations of more than one million to the country's population living in metropolitan areas in percentiles is used, as illustrated in Figure 11. It is found that the correlation can be parametrised with a first order polynomial with a slope of $(1 \pm 0.3) \cdot 10^{-3}$ per day. The significance of the correlation greater than a $3\,\sigma$ Confidence Level. This the most significant correlation out of all the indexes considered here.

4.4. Insights from Outliers

It is appropriate to comment on some of outliers identified in the estimation of α_s in the US. This refers to North Dakota and to a less extent Utah, where $p_{max} = 48, 62$, respectively, are among the lowest in the US. For North Dakota $\alpha_s = 0.018$ and it is the highest in the country. As indicated in Section 4.3, the slope of the exponential growth is sensitive to the fraction of the population living in large cities. None of the above mentioned States have cities with population greater than one million residents. Therefore, these States have been able to keep the rate of growth of positive cases at low enough levels without the implementation of more stringent interventions. This is in contrast to other States where significant portions of their population reside in large cities. In these cases α_s is consistent with the World average from Table 2. A similar picture emerges in South Africa, where two thirds of positive cases are concentrated in the Western Cape and Gauteng Provinces, which host the largest and most densely populated cities in the country.

Some countries, such as Switzerland and most prominently Sweden, have achieved containment without the application of stringent lockdown measures. In these countries citizens are allowed to go out for walks while respecting social distancing. The value of α_s for Sweden is particularly high. Similar reasoning used for the above mentioned US States can be applied here, in that this country lacks large urban agglomerations. It can also be argued that the level of social awareness and observance of social distancing in these countries may play a significant role in the management of the epidemic. It need not be ignored that the prolonged spread of the virus during the early stages of the pandemic in Italy and Spain were driven by lack homogeneity in the adherence to advisories. This prompted governments to introduce severe restrictions to movement, where law enforcement agencies became heavily involved in ensuring compliance. This speaks to the importance of awareness and compliance to increase α_s and with which to reduce the severity of interventions (see Section 4.2).

One is tempted to speculate about the possibility of non-linear behavior in Eq. 2, where could data would favor α_s to increase as p decreases. This would be good news in terms of the effort required to manage the pandemic in that the effectiveness of containment measures could increase as p decreases. This argumentation is hindered by the fact that the lapse of time between changes in the observed non-pharmaceutical interventions was not significant. Measuring the effect of each individual intervention is therefore difficult. As a result of swift action by Governments, we observe the effect of an ensemble of more or less stringent measures, as opposed to their sequential application. To this end, we lack the evidence that would support the above mentioned non-linear behavior. As pointed out in Section 4.2, it is paramount to closely monitor the evolution of α_s as NPIs are released.

4.5. Semi-Empirical Analysis of α_s

It is remarkable that α_s has such a stable value across locales and over these different scales; from states in the US to entire countries $\alpha_s \approx 0.01$. As proof of this assertion, Figure 12 is a depiction of the histogram of α_s values found during our study. There are 2 outliers in the right tail of the plot which have been removed for the remainder of the analysis.

Using $N = 46$ locales and Jeffrey's prior probability[13] for the ensemble variance of α_s, the posterior probability for the ensemble variance, $v = \sigma^2_{\alpha_s}$,

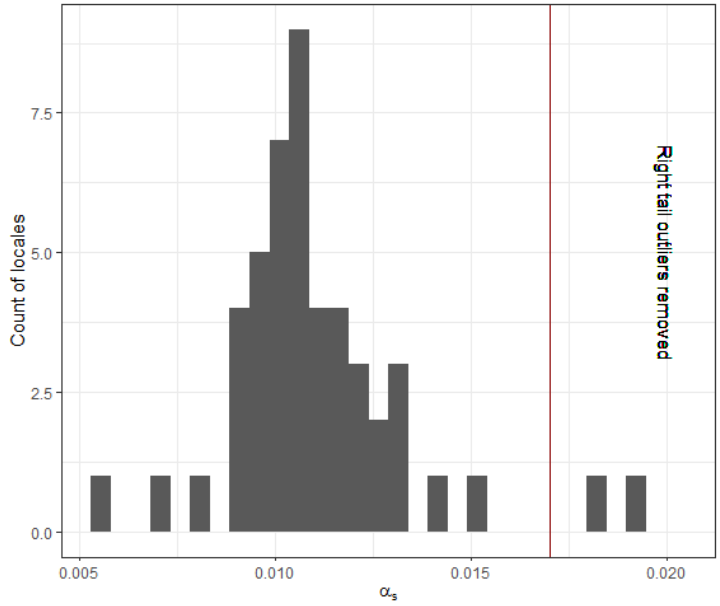

Figure 12: Ensemble of measurements of α_s from Tables 2 and 3.

is given by:

$$\Pr\left(v|\alpha_s[1],\alpha_s[2],...,\alpha_s[N]\right) = \frac{v^{-N/2-1}e^{-\frac{Q}{v}}}{Z}, \tag{9}$$

where

$$Q = \sum_{i=1}^{N} \frac{(\alpha_s[i]-\hat{\mu}_{\alpha_s})^2}{2}, \tag{10}$$

$\hat{\mu}_{\alpha_s}$ is the empirical mean and Z is a normalisation constant. Equation (9) is an inverse gamma distribution and it may be used to calculate the range of probable ensemble variances of α_s across the world, given the sample of locales used in this study.
The results are that the standard deviation of the ensemble σ_{α_s} is 0.0017 (95% CI 0.0014 - 0.0021).

Hence, across 46 countries and states of a wide variety, the sensitivity of these locales to control of the epidemic through NPIs is remarkably well captured by:

$$\alpha_s = 0.01 \pm 0.0017, \tag{11}$$

and, therefore, almost all locales will (in the limit as $p \to 100$) eventually extinguish the epidemic under tight enough control. The outliers which were removed from the analysis show an even greater sensitivity and our models predict that these locales are more easily controlled with softer NPIs.

4.6. Recommendations

There is large existing body of theory on control which may be brought to bare on the present pandemic situation[30,33]. The control engineering literature includes methods to balance the economic effects of various public health initiatives with their likely effect on the epidemic under control and facilitate decision making which is optimal, in a well established mathematical framework[30]. In addition, there are known timing constraints on the rate of control required to keep the epidemic from running away[34]. A metric known as the 'stability margin' is calculable from the known timing constraints and it has implications for how much one can expect to reduce the transmission characteristics when random events disturb the control loop[34]. This calculation and its implications are recommended for another paper to follow the present one.

While lockdown measures have been successful in curbing the spread, our study indicates that removing them too swiftly will result in the resurgence of the spread within one to two months. Reducing the stringency index by 10 will delay reaching the apex by about 6 months, where reducing it by 20 will delay by only four. The amplitude of the apex increases by about a factor of two by moving from $\Delta p = -10$ to $\Delta p = -20$. This indicates that post-lockdown measures should be staged and the reduction of the stringency index should be slow.

Assuming constant γ and d it is essential to increase α_s. For the system to remain sub-critical, the rate with which α_s increases should outpace that of the decrease of the stringency index. Monitoring of α_s becomes essential to controlling the post-lockdown phase.

5. Acknowledgements

Authors are indebted to the South African Department of Science and Innovation and the National Research Foundation for different forms of support. This includes, but it is not limited to, support through the SA-CERN Program and the National E-science Postgraduate Teaching and Training Platform. Authors are also grateful for grant support from the IEEE.

Appendix A. Stringency Index for United States of America

For each policy response measure S1-S7, OxCGRT use the ordinal value (and add one if the policy is general rather than targeted). This creates a score between 0 and 2 and for S5, and 0 and 3 for the other six responses[31].

The OxCGRT stringency index is given by:

$$p = \frac{1}{7}\sum_{J=1}^{7} p_J, \tag{A.1}$$

where p_J is defined by:

$$p_J = \frac{S_J + G_J}{N_J + 1}, \tag{A.2}$$

with $G_J = 1$ if the effect is general (and 0 otherwise), and N_J is the cardinality of the intervention measure[31,32]. In the case where there is no requirement of general vs. targeted (S7), the +1 in the denominator and the G_J in the numerator are omitted from the equation to form:

$$p_7 = \frac{S_7}{N_7}, \tag{A.3}$$

The OxCGRT database contains data for 133 countries however it does not contain specific data for US states. It is important to be able to compare the US states non-pharmaceutical interventions (NPIs) with those of other countries around the World in a unified framework.

To this end, we coded the known levels of intervention in America to match as nearly as possible, the OxCGRT system. We used the Institute for Health Metrics and Evaluation (IHME) dashboard to obtain six dates at which specific states imposed different NPIs[35].

In order to compare the US intervention data it was necessary to make a stringency index for the US states that mimics that of the index that was made for the World data by OxCGRT.

The following decisions were made during the process of mapping the reported US NPIs to the OxCGRT index:

Label	NPI
$U1$:	Stay at Home Order
$U2$:	Educational Facilities Closed
$U3$:	Non-essential Services Closed
$U4$:	Travel Severely Limited
$U5$:	Initial Workplace Closure
$U6$:	Banned Mass Gatherings

Table A.4: Table Showing US Interventions Acquired from the IHME.

- The US *Mass Gatherings Banned* $U5$ can be mapped directly to the Oxford *Cancel Public Events* $S3$.
- The US *Initial Business Closure* $U6$ can be mapped to the Oxford *Work Place Closure* $S2$
- The US *Travel Severely Limited* U_4 can be mapped to the Oxford *Domestic Travel Bans* S6 and *International Travel Bans* S7 combined.

Label	Interventions Not Directly Interchangeable
US NPIs:	
$U1$:	Stay at Home Order
$U3$:	Non-essential Services Closed
OxCGRT NPIs:	
$S4$:	Close Public Transport
$S5$:	Public Information Campaign

Table A.5: Table Showing Unmapped NPIs.

Although some of the above US interventions were not directly comparable to the OxCGRT indicators, their individual impact on the stringency index is still valid and should be included in the index. By including $U1$ and $U3$ with the appropriate weight into the same calculation OxCGRT used for their index, an equivalent US index is created. The following equation was developed:

$$p = \frac{1}{7}(1(v_1) + 1(v_2) + 1(v_3) + 2(v_4) + 1(v_5) + 1(v_6)), \tag{A.4}$$

where v_i is a number out of 100 indicating the extent each of the interventions are imposed.

Due to lack of data on the *Travel Severely Limited* intervention in the IHME database. It was necessary to source US travel restrictions information from other US news sources. There have been a number of travel interventions that have been implemented however there have not been widespread travel bans between states.[36] The first significant travel restriction was a US-Europe travel ban to 26 European countries, which was announced on 11 March 2020.[37] On 19 March 2020 the US issued a level 4 "Do not travel" advisory which is the highest travel restriction in the US. US citizens were informed that they can travel back to the US if they were out of the country when the ban was announced but if they do not do so timely they might find themselves having to stay abroad for an extended period of time. Foreign nationals who have been to the 26 EU countries or the UK, China, Iran or Ireland are not allowed entrance to the US.[38] In terms of the interstate travel restrictions. There have been no full travel bans but in some states you are required to quarantine for 14 days after arrival.[36] Therefore, it was necessary to introduce a leveled implementation of the U4 *Travel Severely Restricted* measure. Using the same logic used by the Oxford COVID-19 Government Response Tracker (OxCGRT) the following equation for v_i was introduced:

$$v_i = 100\frac{U_i}{N_i}, \tag{A.5}$$

where U_i is ordinal and can vary from 0 to the cardinality of the intervention measure, N_i. This is for the purpose of incorporating levels of implementation of specific interventions into the stringency calculation. Based on the data the only intervention that requires levels of implementation is the U_4 intervention.

The following ordinal levels were employed for U_4:

0. No travel restrictions (US before the 11 March 2020)

1. US preliminary travel ban to 26 EU Countries (Commenced 11 March 2020)

2. Level 4 "Do not travel" advisory issued (19 March 2020)

3. Interstate Travel bans (No interstate travel bans are currently imposed)

The specification for comparable p among countries within the OxCGRT database and the United States of America is completed with the above definitions.

Appendix B. Model Details

An explanation of the model is warranted. It has a causal structure and may be clinically interpreted as well, both of which are desirable properties for a model which needs to be controlled[39]. The causal structure gives insight into *what* to control and the clinical interpretation gives insights into *how*.

Susceptible individuals, S : These are the unexposed and susceptible individuals within the population and include healthcare workers as well general members of the public.

Observed infections, I : These infections represent patients who have tested positive for COVID-19 and are actively reported on[11]. Any contacts of these patients who subsequently test positive, any nosocomial infections due to these patients (for example, healthcare workers who contract the disease) or any other individuals who knowingly interact with COVID-19 positive patients are modeled by β, the transmission rate of COVID-19 amongst observed infections. Well prepared countries with strict healthcare protocols for known positive patients, for example quarantining, effective use of personal protective equipment for healthcare providers, and physically separate care pathways for positive patients all essentially work to ensure that β is kept as small as possible.
Asymtpomatic also transmissable Some of these observed infections, I are due to some mild or asymptomatic cases which become severe enough to warrant testing or cause patients to seek medical attention. These cases are modeled by ϕI_L, where ϕ is dependent on the probability that a latent infection I_L becomes a known positive case, I. Latent infections are addressed next.

Latent infections, $\mathbf{I_L}$: There is evidence of a non-trivial fraction of cases going undetected as a result of presenting with mild symptoms or being asymptomatic[40–42]. This is the reason for including the latent variable

dynamics within our modification of the standard SIRD model.
Table 1 in the main text has good estimates of asymptomatic cases; together with the patients who have subclinical manifestations of Covid-19, these cases are all included in the latent infection group, I_L.
It is the susceptible group's interaction with these asymptomatic and mild cases which produce new latent infections and this is modeled through β_L, the non-negligible latent transmission rate.

Latent recoveries, $\mathbf{R_L}$: A majority of these asymptomatic and mild symptom patients resolve the virus using their natural immunity without ever being tested. Early reports indicate that this may be a substantial number of latent infections[17,19]. These cases eventually form part of the latent recovered group, R_L. The rate of recovery of the latent infected group is captured by γ_L.

Latent infections dying, $\delta_L \mathbf{I_L}$: These counts are considered weakly observable and rare. The weak observability is present with the revised, erratic death counts by some officials when home visits uncover additional cases[11]. It is unclear that these may be directly attributable to the virus in that confirmation would be required via post-mortem COVID-19 testing[?] . Given the existing testing burden posed on most countries, this sort of testing is rare and, therefore, the uncertainty in this parameter will remain high[19].

Known recoveries, R : These are patients who are known to test positive for COVID-19 and are known to have recovered fully from the virus. The recovery rate, γ, models how quickly known infections are resolved and discharged out of the healthcare system. This rate is physically dependent on treatment regime and the patient's own physical condition.

Deceased patients, D : The number of deceased individuals is denoted by D; and it is mostly affected by the known individuals who have tested positive and are currently being treated in the prevailing healthcare system. The implications for the model are that $\delta \gg \delta_L$ i.e. under normal treatment and monitoring situations, the implied probability of fatality for a known infection is much larger than the implied probability of fatality for a latent infection.
Under the above conditions, the model explicitly caters explicitly for the situation that the latent infections are asymptomatic or mild.
It is trivial to show that $S + I + I_L + R_L + R + D = N$ at every instant

in time. Furthermore, the model in Figure 1 implies that:

$$\frac{\mathrm{d}S}{\mathrm{d}t} = -\beta_L \frac{S\, I_L}{N}, \tag{B.1}$$

$$\frac{\mathrm{d}I_L}{\mathrm{d}t} = \beta_L \frac{S\, I_L}{N} - \phi\, I_L - \gamma_L\, I_L, \tag{B.2}$$

$$\frac{\mathrm{d}I}{\mathrm{d}t} = \phi I_L - \delta\, I - \gamma\, I, \tag{B.3}$$

$$\frac{\mathrm{d}R}{\mathrm{d}t} = \gamma\, I, \tag{B.4}$$

$$\frac{\mathrm{d}D}{\mathrm{d}t} = \delta\, I. \tag{B.5}$$

Appendix B.1. Linearisation

Each of the equations in (B.1) - (B.5) were linearised using the approximation that $S = N - \epsilon$, which gives equivalent results to the Jacobian method[28]. This operating point corresponds to the case where the epidemic is still in the early/controllable phase and the number of infected individuals is small compared with the size of the total population N.
The derivatives with respect to time were approximated using first order backward difference approximations at a daily level. Classical frequentist error propagation was applied to this linear approximation using the Gaussian process assumption.
Theoretically, these approximations are valid provided that:

1. the number of infected are a small fraction of the susceptible population.

2. the dynamics of the disease process are slow compared with a single day. This is justified by the work from Weiss and Murdoch[42].

The final form, used for analysis of the time variation of the parameters as various forms of control are applied is:

$$\gamma(t) = \frac{\Delta R}{I[t-1]} \pm \sigma_\gamma(t), \tag{B.6}$$

$$\delta(t) = \frac{\Delta D}{I[t-1]} \pm \sigma_\delta(t), \tag{B.7}$$

$$\beta(t) = \frac{\Delta R + \Delta D + \Delta I}{I[t-1]} \pm \sigma_\beta(t), \tag{B.8}$$

where $\sigma_x(t)$ is the noise estimate at day t, $\Delta x := x[t] - x[t-1]$ and x is either R, D or I.

Appendix B.2. Error propagation

Using the coefficient of variation and propagating the error in the linear approximation, assuming that the errors in the daily counts are within 10% [43], the probable noise levels in the daily time variations are calculated by:

$$\sigma_\gamma(t) = \gamma(t)\sqrt{\frac{1}{\Delta R} + \frac{1}{I[t-1]}}, \tag{B.9}$$

$$\sigma_\beta(t) = \beta(t)\sqrt{\frac{1}{\Delta R + \Delta I + \Delta D} + \frac{1}{I[t-1]}}, \tag{B.10}$$

and

$$\sigma_\delta(t) = \delta(t)\sqrt{\frac{1}{\Delta D} + \frac{1}{I[t-1]}}. \tag{B.11}$$

These results depend on the count data being Poisson processes and the fact that the coefficient of variation of a Poisson process is $\lambda^{-1/2}$. Recall that the general coefficient of variation of a division of two random variables is the quadrature sum of the numerator and denominator coefficients of variation; the results follow [43].

Appendix C. Details of Linearisation

If dt is taken as one day, t is the day index and $\Delta x = x[t] - x[t-1]$, then with the modeling assumptions the differential equations simplify to:

$$\Delta S = -\beta_L \, I_L[t-1], \tag{C.1}$$

$$\Delta I_L = (\beta_L - \gamma_L - \phi) \, I_L[t-1], \tag{C.2}$$

$$\Delta I = \phi\, I_L[t-1] - \gamma\, I[t-1] - \delta\, I[t-1], \tag{C.3}$$

$$\Delta R = \gamma\, I[t-1], \tag{C.4}$$

$$\Delta D = \delta\, I[t-1]. \tag{C.5}$$

Use of (C.4) and (C.5) yield the daily estimates of the observable recovery rate, γ and fatality rate δ. Combining (C.4), (C.5) and (C.3) give the daily estimate of the transmission rate, as observed through the detection efficiency.

Appendix C.1. Control Dynamics

Efforts to control the pandemic do not happen everywhere, all at once and this is the reason that the control efforts can be said to be dynamic. Indeed, the form of the kernel functions in equations (1) - (4) state this implicitly. Each of the observed parameters will be looked at it in this section and their dynamics described. These forms have non-trivial implications for control of the pandemic and will be expounded upon in a follow up paper.

Transmission rate

The beta kernel in (1) and the steady state behaviour modeled by (2) imply that the transmission dynamics, under stringency of control p, behave as a first order control system[28]:

$$b_r \frac{\mathrm{d}\beta}{\mathrm{d}t} = \beta_0 - \beta(t) - \beta_0 \alpha_s p, \tag{C.6}$$

where b_r is the typical adjustment time for a control measure to take full effect, α_s is the societal sensitivity (estimated for each country in our work) to control measures $p \in [0, 100]$, and β_0 is the uncontrolled transmission rate within a society.

As a sense check; when $p = 0$ then the equilibrium condition of (C.6) is found by solving (C.6) with $\beta(t) = \beta_f = const$. The non-trivial solution is $\beta_f = \beta_0$ and shows that, without control, the transmission rate becomes β_0. This is defined as the uncontrolled transmission rate and is as it should be.

If $p \neq 0$, then the equilibrium condition is $\beta_f = \beta_0 - \beta_0 \alpha_s p$ which is exactly equation (2). The general analytic solution to (C.6) is precisely the kernel function in (1).

It is this form which allows for the use of classic and modern control methods to shape $\beta(t)$ to a form that is acceptable for the desired goals of the pandemic control system eg. minimise total deaths, minimise the peak load on the health care system, maximise the economic activity etc. These aspects will be dealt with in detail in a follow up paper.

References

[1] W.H.O, Who director-general's opening remarks at the media briefing on covid-19 - 11 march 2020, online https://www.who.int/dg/speeches/detail/who-director-general-s-opening-remarks-at-the-media-briefing-on-covid-19—11-march-2020, accessed 25 Apr, 2020.

[2] W.H.O, Coronavirus disease 2019 (covid-19) situation report 89 - 18 april 2020, online https://www.who.int/emergencies/diseases/novel-coronavirus-2019/situation-reports, accessed 19 Apr, 2020.

[3] S. Flaxman, S. Mishra, A. Gandy, H. Unwin, H. Coupland, T. Mellan, H. Zhu, T. Berah, J. Eaton, P. Perez Guzman, N. Schmit, L. Cilloni, K. Ainslie, M. Baguelin, I. Blake, A. Boonyasiri, O. Boyd, L. Cattarino, C. Ciavarella, L. Cooper, Z. Cucunuba Perez, G. Cuomo-Dannenburg, A. Dighe, A. Djaafara, I. Dorigatti, S. Van Elsland, R. Fitzjohn, H. Fu, K. Gaythorpe, L. Geidelberg, N. Grassly, W. Green, T. Hallett, A. Hamlet, W. Hinsley, B. Jeffrey, D. Jorgensen, E. Knock, D. Laydon, G. Nedjati Gilani, P. Nouvellet, K. Parag, I. Siveroni, H. Thompson, R. Verity, E. Volz, C. Walters, H. Wang, Y. Wang, O. Watson, P. Winskill, X. Xi, C. Whittaker, P. Walker, A. Ghani, C. Donnelly, S. Riley, L. Okell, M. Vollmer, N. Ferguson, S. Bhatt, Report 13: Estimating the number of infections and the impact of non-pharmaceutical interventions on covid-19 in 11 european countries (2020).

[4] K. Leung, J. T. Wu, D. Liu, G. M. Leung, First-wave covid-19 transmissibility and severity in china outside hubei after control measures, and second-wave scenario planning: a modelling impact assessment, The Lancet (2020).

[5] R. M. Anderson, H. Heesterbeek, D. Klinkenberg, T. D. Hollingsworth, How will country-based mitigation measures influence the course of the covid-19 epidemic?, The Lancet 395 (2020) 931–934.

[6] J. Hellewell, S. Abbott, A. Gimma, N. I. Bosse, C. I. Jarvis, T. W. Russell, J. D. Munday, A. J. Kucharski, W. J. Edmunds, S. Funk, R. M. Eggo, F. Sun, S. Flasche, B. J. Quilty, N. Davies, Y. Liu, S. Clifford, P. Klepac, M. Jit, C. Diamond, H. Gibbs, K. van Zandvoort, Feasibility of controlling covid-19 outbreaks by isolation of cases and contacts, The Lancet Global Health 8 (2020) e488–e496.

[7] N. Ferguson, D. Laydon, G. Nedjati Gilani, N. Imai, K. Ainslie, M. Baguelin, S. Bhatia, A. Boonyasiri, Z. Cucunuba Perez, G. Cuomo-Dannenburg, A. Dighe, I. Dorigatti, H. Fu, K. Gaythorpe, W. Green, A. Hamlet, W. Hinsley, L. Okell, S. Van Elsland, H. Thompson, R. Verity, E. Volz, H. Wang, Y. Wang, P. Walker, P. Winskill, C. Whittaker, C. Donnelly, S. Riley, A. Ghani, Report 9: Impact of non-pharmaceutical interventions (npis) to reduce covid19 mortality and healthcare demand (2020).

[8] J. M. Gardner, L. Willem, W. van der Wijngaart, S. C. L. Kamerlin, N. Brusselaers, P. Kasson, (medrxiv preprint) intervention strategies against covid-19 and their estimated impact on swedish healthcare capacity (2020).

[9] K. Prem, Y. Liu, T. W. Russell, A. J. Kucharski, R. M. Eggo, N. Davies, M. Jit, P. Klepac, S. Flasche, S. Clifford, C. A. B. Pearson, J. D. Munday, S. Abbott, H. Gibbs, A. Rosello, B. J. Quilty, T. Jombart, F. Sun, C. Diamond, A. Gimma, K. van Zandvoort, S. Funk, C. I. Jarvis, W. J. Edmunds, N. I. Bosse, J. Hellewell, The effect of control strategies to reduce social mixing on outcomes of the covid-19 epidemic in wuhan, china: a modelling study, The Lancet Public Health (2020).

[10] B. J. Cowling, S. T. Ali, T. W. Y. Ng, T. K. Tsang, J. C. M. Li, M. W. Fong, Q. Liao, M. Y. Kwan, S. L. Lee, S. S. Chiu, J. T. Wu, P. Wu, G. M. Leung, Impact assessment of non-pharmaceutical interventions against coronavirus disease 2019 and influenza in hong kong: an observational study, The Lancet Public Health (2020).

[11] E. Dong, H. Du, L. Gardner, An interactive web-based dashboard to track covid-19 in real time, The Lancet Infectious Diseases (2020).

[12] T. Hale, A. Petherick, T. Phillips, S. Webster, Variation in government responses to covid-19, bsg-wp-2020/031 4.0, 2020.

[13] E. T. Jaynes, Probability theory : the logic of science, Cambridge University Press, Cambridge, UK New York, NY, 2003.

[14] N. Taleb, The Black Swan : The Impact of the Highly Improbable, Random House, New York, 2007.

[15] R. Verity, L. C. Okell, I. Dorigatti, P. Winskill, C. Whittaker, N. Imai, G. Cuomo-Dannenburg, H. Thompson, P. G. T. Walker, H. Fu, A. Dighe, J. T. Griffin, M. Baguelin, S. Bhatia, A. Boonyasiri, A. Cori, Z. Cucunubá, R. FitzJohn, K. Gaythorpe, W. Green, A. Hamlet, W. Hinsley, D. Laydon, G. Nedjati-Gilani, S. Riley, S. van Elsland, E. Volz, H. Wang, Y. Wang, X. Xi, C. A. Donnelly, A. C. Ghani, N. M. Ferguson, Estimates of the severity of coronavirus disease 2019: a model-based analysis, The Lancet Infectious Diseases (2020).

[16] S. Law, A. W. Leung, C. Xu, Severe acute respiratory syndrome (SARS) and coronavirus disease-2019 (COVID-19): From causes to preventions in hong kong, International Journal of Infectious Diseases (2020).

[17] D. F. Gudbjartsson, A. Helgason, H. Jonsson, O. T. Magnusson, P. Melsted, G. L. Norddahl, J. Saemundsdottir, A. Sigurdsson, P. Sulem, A. B. Agustsdottir, B. Eiriksdottir, R. Fridriksdottir, E. E. Gardarsdottir, G. Georgsson, O. S. Gretarsdottir, K. R. Gudmundsson, T. R. Gunnarsdottir, A. Gylfason, H. Holm, B. O. Jensson, A. Jonasdottir, F. Jonsson, K. S. Josefsdottir, T. Kristjansson, D. N. Magnusdottir, L. le Roux, G. Sigmundsdottir, G. Sveinbjornsson, K. E. Sveinsdottir, M. Sveinsdottir, E. A. Thorarensen, B. Thorbjornsson, A. Löve, G. Masson, I. Jonsdottir, A. D. Möller, T. Gudnason, K. G. Kristinsson, U. Thorsteinsdottir, K. Stefansson, Spread of SARS-CoV-2 in the icelandic population, New England Journal of Medicine (2020).

[18] Cdc guidance for certifying covid-19 deaths, online https://www.cdc.gov/nchs/data/nvss/coronavirus/Alert-1-Guidance-for-Certifying-COVID-19-Deaths.pdf, accessed 27 April, 2020.

[19] New york releases antibody testing data: 14% of population may be infected with coronavirus, online https://eu.usatoday.com/story/news/nation/2020/04/23/coronavirus-new-york-millions-residents-may-have-been-infected-antibody-test/3012920001/, accessed 27 April, 2020.

[20] T. Lancet, COVID-19: protecting health-care workers, The Lancet 395 (2020) 922.

[21] S.-Y. Wong, R.-S. Kwong, T. Wu, J. Chan, M. Chu, S. Lee, H. Wong, D. Lung, Risk of nosocomial transmission of coronavirus disease 2019: an experience in a general ward setting in hong kong, Journal of Hospital Infection (2020).

[22] Y. Shi, Y. Wang, C. Shao, J. Huang, J. Gan, X. Huang, E. Bucci, M. Piacentini, G. Ippolito, G. Melino, COVID-19 infection: the perspectives on immune responses, Cell Death & Differentiation 27 (2020) 1451–1454.

[23] Y. Liu, L.-M. Yan, L. Wan, T.-X. Xiang, A. Le, J.-M. Liu, M. Peiris, L. L. M. Poon, W. Zhang, Viral dynamics in mild and severe cases of COVID-19, The Lancet Infectious Diseases (2020).

[24] M. Day, Covid-19: identifying and isolating asymptomatic people helped eliminate virus in italian village, BMJ (2020) m1165.

[25] H. Nishiura, T. Kobayashi, A. Suzuki, S.-M. Jung, K. Hayashi, R. Kinoshita, Y. Yang, B. Yuan, A. R. Akhmetzhanov, N. M. Linton, T. Miyama, Estimation of the asymptomatic ratio of novel coronavirus infections (COVID-19), International Journal of Infectious Diseases (2020).

[26] A. Kimball, K. M. Hatfield, M. Arons, A. James, J. Taylor, K. Spicer, A. C. Bardossy, L. P. Oakley, S. Tanwar, Z. Chisty, J. M. Bell, M. Methner, J. Harney, J. R. Jacobs, C. M. Carlson, H. P. McLaughlin, N. Stone, S. Clark, C. Brostrom-Smith, L. C. Page, M. Kay, J. Lewis, D. Russell, B. Hiatt, J. Gant, J. S. Duchin, T. A. Clark, M. A. Honein, S. C. Reddy, J. A. Jernigan, A. Baer, L. M. Barnard, E. Benoliel, M. S. Fagalde, J. Ferro, H. G. Smith, E. Gonzales, N. Hatley, G. Hatt, M. Hope, M. Huntington-Frazier, V. Kawakami, J. L. Lenahan, M. D. Lukoff, E. B. Maier, S. McKeirnan, P. Montgomery, J. L. Morgan, L. A. Mummert, S. Pogosjans, F. X. Riedo, L. Schwarcz, D. Smith, S. Stearns, K. J. Sykes, H. Whitney, H. Ali, M. Banks, A. Balajee, E. J. Chow, B. Cooper, D. W. Currie, J. Dyal, J. Healy, M. Hughes, T. M. McMichael, L. Nolen, C. Olson, A. K. Rao, K. Schmit, N. G. Schwartz, F. Tobolowsky, R. Zacks, S. Zane, , , and, Asymptomatic and presymptomatic SARS-CoV-2 infections in residents of a long-term care skilled nursing facility — king

856 county, washington, march 2020, MMWR. Morbidity and Mortality
857 Weekly Report 69 (2020) 377–381.

858 [27] Coronavirus, castiglione d'adda è un caso di studio: 'il 70% dei donatori
859 di sangue è positivo', online https://www.lastampa.it/topnews/primo-
860 piano/2020/04/02/news/coronavirus-castiglione-d-adda-e-un-caso-di-
861 studio-il-70-dei-donatori-di-sangue-e-positivo-1.38666481, accessed 27
862 April, 2020.

863 [28] K. Astrom, M. Murray, Feedback systems : an introduction for scientists
864 and engineers, Princeton University Press, Princeton, 2008.

865 [29] N. Kandel, S. Chungong, A. Omaar, J. Xing, Health security capacities
866 in the context of covid-19 outbreak: an analysis of international health
867 regulations annual report data from 182 countries, The Lancet 395
868 (2020) 1047–1053.

869 [30] C. Nowzari, V. M. Preciado, G. J. Pappas, Analysis and control of
870 epidemics: A survey of spreading processes on complex networks, IEEE
871 Control Systems Magazine 36 (2016) 26–46.

872 [31] Oxford coronavirus government response tracker, online
873 https://www.bsg.ox.ac.uk/research/research-projects/coronavirus-
874 government-response-tracker, accessed 14 April, 2020.

875 [32] University of oxford, calculation and presen-
876 tation of the stringency index 2.0, online
877 https://www.bsg.ox.ac.uk/sites/default/files/Calculation%20and
878 %20presentation%20of%20the%20Stringency%20Index.pdf, accessed 14
879 April, 2020.

880 [33] K. Lin, F.and Muthuraman, M. Lawley, An optimal control theory
881 approach to non-pharmaceutical interventions, BMC Infectious Diseases
882 10 (2010).

883 [34] G. Stein, Respect the unstable, IEEE Control Systems Magazine 23
884 (2003) 12–25.

885 [35] University of washington, institute for health metrics and evaluation
886 covid-19 projections, 2020.

[36] K. Schwartz, Driving and travel restrictions across the united states, 2020.

[37] P. Baker, U.s. to suspend most travel from europe as world scrambles to fight pandemic, 2020.

[38] A. Salcedo, S. Yar, G. Cherelus, Coronavirus travel restrictions, across the globe, 2020.

[39] R. McElreath, Statistical rethinking : a Bayesian course with examples in R and Stan, Chapman & Hall/CRC, Boca Raton, 2020.

[40] A. Haines, E. F. de Barros, A. Berlin, D. L. Heymann, M. J. Harris, National UK programme of community health workers for covid-19 response, The Lancet 395 (2020) 1173–1175.

[41] H. V. Fineberg, Ten weeks to crush the curve, New England Journal of Medicine (2020).

[42] P. Weiss, D. R. Murdoch, Clinical course and mortality risk of severe covid-19, The Lancet 395 (2020) 1014–1015.

[43] D. T. Holmes, K. A. Buhr, Error propagation in calculated ratios, Clinical Biochemistry 40 (2007) 728–734.